Reactive & Functional Polymers 82 (2014) 17–24

Contents lists available at ScienceDirect

Reactive & Functional Polymers

journal homepage: www.elsevier.com/locate/react

Optically active amino acid-based polyacetylenes: Effect of tunable helical conformation on infrared emissivity property

Xiaohai Bu, Yuming Zhou *, Zhenjie Chen, Man He, Tao Zhang

School of Chemistry and Chemical Engineering, Southeast University, Jiangsu Optoelectronic Functional Materials and Engineering Laboratory, Nanjing 211189, PR China

ARTICLE INFO

Article history:
Received 22 September 2013
Received in revised form 10 January 2014
Accepted 15 May 2014
Available online 27 May 2014

Keywords:
Amino acid
Polyacetylenes
Helical conformation
Intramolecular hydrogen bonds
Infrared emissivity

ABSTRACT

Chiral amino acid-based monosubstituted acetylene monomers [*N*-*tert*-butoxy-carbonyl-L-phenylalanine-*N*′-propargylamide (LP), and *N*-*tert*-butoxycarbonyl-L-serine-*N*′-propargylamide (LS)] were (co)polymerized with rhodium zwitterion catalyst in THF to afford helical polyacetylenes (PAs) with moderate molecular weights (4400–14,800) in good yields. The optically active PA copolymers were soluble in common organic solvents and proven to adopt predominately single-handed helical conformations according to their intense Cotton effect and large specific rotations. Various contents of amino acid units in side chains facilitated controllable helical secondary structure while the helix was primarily stabilized by hydrogen bonding and steric repulsion between the substituents. Intramolecular hydrogen bonds constructed between hydroxyl and amide groups, in particular, played a significant role in adjusting the helicity and orderliness of the helix. The infrared emissivity values of the PAs at wavelength of 8–14 μm were measured and the correlation between helical conformations and their effect on infrared emission were systematically investigated. The results showed that more well-ordered and compact screw-sense could enhance the performance of organic polymers in lowering their infrared emissivity. Among all the as-prepared PAs, poly(LP_{50}-*co*-LS_{50}) exhibited the lowest infrared emissivity value (ε_{25} = 0.632) and possessed excellent resistance against heat.

1. Introduction

Materials with tunable infrared emissivity have attracted widespread attention due to their importance in both thermal insulation and military stealthy [1–3]. Various inorganic or metallic materials have been widely used to achieve low emissivity because of their high reflectance in infrared waveband [4,5]. Organic polymers containing highly absorptive chemical bonds, e.g. C—H, C=O, N—H, etc., result in relatively high emissivity (commonly larger than 0.90) [6–9], which limit their applications in low-emissivity field. However, organic polymers possess unique properties including low density, tractability, anti-corrosion and the most value, their adjustable composition and structure, which can provide the possibility of adjusting their emission performance efficaciously according to practical applications. Thus, it has still remained a meaningful research objective to develop novel classes of organic polymers with tunable infrared emissivity.

Special interest in helical polymers arises from the realization that their high-ordered stereoregular structure is essential in maintaining their usual properties. Helix is one of the most common structures in naturally occurring biomacromolecules as well as in synthetic polymers. Helices are primarily constructed through intra- and/or intermolecular associations by noncovalent forces, such as hydrogen bonding, hydrophobic-stacking, and electrostatic interactions [10]. Helix means molecularly asymmetric; hence, the polymer chain will prefer predominantly a single-handed screw sense and exert optical activity [11]. For numerous synthetic helical polymers, conformational transition can lead to interesting changes in their physical and chemical properties, thus providing opportunities to develop smart and intelligent macromolecules [12–14]. Recently, in the case of organic polymers with tunable infrared emissivity, considerable effort has been devoted to applying helical polymers in this field owing to their adjustable secondary structure. For example, Wang et al. [15] firstly reported that optically active polyurethane-urea had a lower infrared emissivity value compared with racemic polymers owing to its ordered single-handed conformation. Yang et al. [16,17] prepared optically active polyurethanes with enhanced performance in lowering emissivity values and further studied the correlation between the helical structure and its effect on infrared emission. According to the previous works, well-ordered structure seems to be efficient in decreasing the infrared emissivity, in spite of the presence of

* Corresponding author. Tel./fax: +86 25 52090617.
E-mail address: ymzhou@seu.edu.cn (Y. Zhou).

http://dx.doi.org/10.1016/j.reactfunctpolym.2014.05.006
1381-5148/

unfavorable absorptive groups in synthetic polymers. As we know, the vibration of unsaturated functional groups in synthetic polymers mainly brings about high infrared radiation. Theoretically, more compact accumulation of fragments and orderly inter- and intramolecular interactions will accelerate the changing of vibrational state of unsaturated bonds and thermal restraining in backbones, which can largely influence the infrared emission performance [15,16,18]. Namely, a high-ordered secondary structure in the helical polymer, to some extent, can change the vibration mode in the whole macromolecular to reduce the index of hydrogen deficiency and the unsaturated degree, thus eventually facilitating the remarkable decrease in infrared emissivity values.

Substituted polyacetylenes are prototypical π-conjugated polymers and exhibit interesting properties and functions, including liquid crystallinity [19], photoconductivity [20], luminescence [21], gas permeability [22], and asymmetric catalysis [23]. They possess alternating double bonds along the main chain, in which the conjugation significantly depends on the type, number, and bulkiness of the pedants [24–26]. To date, monosubstituted PAs bearing amino acid moieties in the side chains has been the subject of study, because amino acid endows them with new features originating from their inherent chirality, diverse groups and ability to form hydrogen bonds. The introduction of appropriate amino acid-based moieties to the side chains easily induces them to take regulated higher order structure. A wide variety of helical PAs derived from chiral amino acid have been designed and synthesized. Masuda et al. [27–29] synthesized PAs derived from various amino acids and discussed their conformational transition by changing temperature and solvent. Tang and co-workers focused on helical poly(phenylacetylenes) carrying amino acid moieties, some of which exhibit attractive properties including forming helical nanofibers [30,31], self-assembling [32], and tuning the helicity by pH change [33]. These PAs form helices stabilized by hydrogen bonding along with steric repulsion, while whose sense, tightness, and stability depend on the functional groups in the pendants such as amide, hydroxyl, and aromatic groups. Especially, hydroxyl group forms hydrogen bonding in a different way which can not only assist the formation of hydrogen bonds but also adjust the helicity and stability of the helix [34]. In fact, participation of hydroxyl group in intramolecular hydrogen bonding changes the torsional angles in the main chain, which largely affects the conformation and property of the PAs [35,36]. This finding is highly significant for further designing amino acid-based PAs with tunable helical conformation for special applications, for instance, helical PAs for low infrared emissivity application.

To the best of our knowledge, there are few reports dealing with the copolymerization of hydroxyl group containing amino acid PAs and the analyses about their conformation are rare. Besides, there are also few reports concerning the application of helical polymers to achieve tunable infrared emissivity, let alone helical PAs. Herein, a series of PAs derived from L-phenylalanine and L-serine was designed and synthesized. Phenyl rings in LP are incorporated into the PA backbone with the hope that the bulky moieties exert asymmetric forces to induce the chain to take a compact helical conformation, while hydroxyl groups in LS are incorporated for the helicity and stability tuning. As the structurally composition of the chiral monomers varies, the change of the degree of hydrogen bonding and steric interactions in the PAs can generate differing quantities of steric configuration in macromolecules. Thence, it can be expected that the optimization of the helicity and orderliness of the polymer chains can afford novel PAs with enhanced performance in controlling infrared emission. Furthermore, after examining the infrared emissivity values of the PAs, we try to capture the relationship of the secondary structure, hydrogen bonding and the infrared emissivity of the PAs in an effort to study their potential applications.

2. Experimental section

2.1. Materials

Propargylamine, *N-tert*-butoxycarbonyl-L-phenylalanine and *N-tert*-butoxycarbonyl-L-serine were purchased from Aladdin. Isobutyl chloroformate and 4-methymorpholine were purchased from Sinopharm Chemical Reagent Co., Ltd. (nbd)$Rh^+[\eta^6$-$C_6H_5B^-(C_6H_5)_3]$ (nbd = 2,5-norbornadiene) was prepared by the reaction of $[(nbd)RhCl]_2$ with $NaB(C_6H_5)_4$ as reported [37]. THF used for polymerization was distilled over CaH_2 prior to use. All other regents were used as received without further purification.

2.2. Measurements

Melting point (mp) was measured by an X-4 micro-melting point apparatus. Solid and solution state FT-IR spectra were carried out on a Bruker Tensor 27 FT-IR spectrometer at room temperature using KBr pellets and a KBr liquid cell, respectively. The spectra were obtained at a 4 cm^{-1} resolution and recorded in the region of 4000–400 cm^{-1}. ^1H and ^{13}C NMR spectra measurements were recorded on a Bruker AVANCE 300 NMR spectrometer. Chemical shifts were reported in ppm. The molecular weights and molecular weight polydispersities were estimated by gel permeation chromatography (Shodex KF-850 column, THF as the eluent, polystyrene calibration). UV–vis spectra were measured on a Shimadzu UV-3600 spectrometer. CD spectra were determined with a Jasco J-810 spectropolarimeter using a 10 mm quartz cell at room temperature. Specific rotations ($[\alpha]_D$) were measured in a WZZ-2S (2SS) digital automatic polarimeter at room temperature. Thermal analysis experiments were performed using a TGA apparatus operated in the conventional TGA mode (TA Q-600, TA Instruments) at a heating rate of 10 K min^{-1} in a nitrogen atmosphere, and the sample size was about 5 mg. The infrared emissivity values (ε) of polymers at wavelength of 8–14 μm were investigated on the IRE-2 Infrared Emissometer of Shanghai Institute of Technology and Physics, China. Infrared emissivity values of the samples at 30–160 °C were recorded with a temperature control instrument at a heating rate of 5 K min^{-1}.

2.3. Monomer synthesis

2.3.1. *N-tert-butoxycarbonyl-L-phenylalanine-N′-propargylamide (LP)*

N-tert-butoxycarbonyl-L-phenylalanine (1.46 g, 5.5 mmol), isobutyl chloroformate (0.72 mL, 5.5 mmol) and 4-methymorpholine (0.6 mL, 5.5 mmol) were sequentially added into 35 mL THF. The solution was stirred at room temperature for about 15 min and then propargylamine (0.303 g, 5.5 mmol) was added into the solution. The resulting mixture was stirred at room temperature for 24 h. The white precipitate was filtered off, and then the filtrate was collected, to which AcOEt (200 mL) was added to extract the desired product. The combined solution was subsequently washed with 1 M HCl (three times), saturated aq. $NaHCO_3$, saturated aq. NaCl, dried over anhydrous $MgSO_4$ and concentrated by rotary evaporation. The residue was purified by flash column chromatography on silica gel eluted with *n*-hexane/AcOEt (2/1, v/v) to obtain solid monomer. Yield = 84%, white solid powder, mp: 102 °C. $[\alpha]_D = -3.5°$ (c = 0.1 g dL^{-1}, THF, rt). FT-IR (cm^{-1}, KBr): 3326, 1690, 1655, 1529, 1446, 1390, 1367, 1271, 1091, 1049, 1027, 855, 758, 702, 668, 577, 513. ^1H NMR (300 MHz, $CDCl_3$): δ 1.42 [s, 9H, $(CH_3)_3$], 2.21 (s, 1H, C≡C*H*), 3.09 (s, 2H, CHCH_2), 4.00 (s, 2H, CH_2NH), 4.36 (s, 1H, H_3CC*H*NH), 5.05 (s, 1H, N*H*COO), 6.17 (1H, N*H*CO), 7.22–7.31 (m, 5H, $CH_2C_6H_5$). ^{13}C NMR (75 MHz, $CDCl_3$): δ 28.30, 29.03, 38.73, 55.64, 71.58, 79.21, 80.17, 126.86, 128.56, 129.38, 136.36, 155.60, 171.42.

2.3.2. N-tert-butoxycarbonyl-L-serine-N′-propargylamide (LS)

The title compound was synthesized from *N*-*tert*-butoxycarbonyl-L-serine in a manner similar to the synthesis of LP. Yield = 62%, colorless crystal, mp: 156–158 °C. $[\alpha]_D = 5.9°$ ($c = 0.1$ g dL^{-1}, THF, rt). FT-IR (cm^{-1}, KBr): 3454, 3330, 3303, 3096, 1710, 1662, 1570, 1536, 1410, 1365, 1283, 1249, 1174, 1058, 1046, 930, 863, 785, 659, 526. ^{1}H NMR (300 MHz, $CDCl_3$): δ 1.49 [s, 9H, $(CH_3)_3$], 2.20 (s, 1H, C≡C*H*), 2.91 (s, 1H, CH_2OH), 3.69 (s, 1H, CH_2CHNH), 4.09 (s, 2H, $CHCH_2OH$), 4.16 (m, 2H, CH_2NH), 5.60(s, 1H, CHN*H*CO), 7.02 (s, CH_2NHCO). ^{13}C NMR (75 MHz, $CDCl_3$): δ 28.30, 29.35, 56.50, 62.89, 71.74, 79.03, 80.99, 157.82, 171.28.

2.4. Polymerization

Polymerizations were carried out in a Y-shaped glass tube equipped with a three-way stopcock under nitrogen. Monomers and (nbd)Rh$^+$[η^6-$C_6H_5B^-(C_6H_5)_3$] ([initial monomers] = 0.5 M, [catalyst] = 5 mM) were respectively dissolved in THF under N_2 atmosphere. Then the monomers and catalyst were mixed and stirred at 30 °C for 12 h. After polymerization, the resultant solution was added dropwise into a large amount of hexane/AcOEt (10/1, v/v) to precipitate the formed polymers. The precipitate was collected by filtration and dried under reduced pressure to obtain the PAs product. Polymers synthesized by proportional feed ratio of LP and LS are listed in Table 1. The spectroscopic data of poly(LP), poly(LP_{50}-*co*-LS_{50}) and poly(LS) are shown as follows:

Poly(LP) FT-IR (cm^{-1}, KBr): 3347, 3260, 3086, 2978, 2929, 1692, 1653,1578, 1519, 1457, 1396, 1368, 1247, 1171, 1050, 1017, 858, 750, 700; ^{1}H NMR (300 MHz, $CDCl_3$): δ 1.44 [br, 9H, $(CH_3)_3$], 2.6–5.0 (m, $CHCH_2$, CH_2NH, H_3CCHNH), 5.05 (s, 1H, N*H*COO), 5.53 (s, 1H, C=C*H*), 6.58 (1H, N*H*CO), 7.29 (m, 5H, $CH_2C_6H_5$); poly(LP_{50}-*co*-LS_{50}) FT-IR (cm^{-1}, KBr): 3423, 3324, 3084, 2978, 2930, 1699, 1662, 1518, 1456, 1395, 1367, 1250, 1165, 1061, 1021, 853, 787, 751, 701; ^{1}H NMR (300 MHz, $CDCl_3$): δ 1.44 [br, 18H, $(CH_3)_3$], 2.3–2.70 (br, 1H, CH_2OH), 3.0–5.0 (m, 10H, CH_2CHNH, $CHCH_2OH$, CH_2NH), 5.44–6.90 (m, 4H, CHN*H*CO, C=C*H*), 7.30 (m, 5H, $CH_2C_6H_5$), 8.04 (br, 2H, CH_2NHCO); poly(LS) FT-IR (cm^{-1}, KBr): 3600–3200, 3006, 2980, 2930, 2884, 1698, 1658, 1523, 1459, 1399, 1367, 1256, 1169, 1065, 918, 858, 782, 591; ^{1}H NMR (300 MHz, $CDCl_3$): δ 1.45 [br, 9H, $(CH_3)_3$], 2.5–3.0 (br, 1H, CH_2OH), 3.1–5.0 (m, 5H, CH_2CHNH, $CHCH_2OH$, CH_2NH), 6.10 (br, 2H, CHN*H*CO, C=C*H*), 8.07 (br, 1H, CH_2NHCO).

The FT-IR and ^{1}H NMR data of other copolymers are similar to poly(LP_{50}-*co*-LS_{50}) and shown in Figs. S1 and S2.

Table 1
Copolymerization of LP with LS[a].

Monomer feed ratio (LP:LS)	Yield[b] (%)	M_n[c]	M_w/M_n	$[\alpha]_D$[d] (°)	
				$CHCl_3$	MeOH
100:0	88	4400	1.3	[e]	[e]
75:25	94	10,500	1.9	−120	−36
62.5:37.5	98	14,800	1.6	−229	−60
50:50	96	14,200	2.0	−386	−93
37.5:62.5	95	11,100	1.9	−285	−220
25:75	90	10,700	1.8	−204	−281
0:100	80	9900	2.3	−152	−456

[a] Conditions: catalyst (nbd)Rh$^+$[η^6-$C_6H_5B^-(C_6H_5)_3$], [monomer]/[catalyst] = 100, at 30 °C for 24 h under N_2.
[b] Insoluble part in n-hexane/AcOEt (10/1, v/v).
[c] Determined by GPC eluted with THF based on polystyrene standards.
[d] Measured in $CHCl_3$ and MeOH by polarimetry at room temperature, $c = 0.05$ g dL^{-1}.
[e] Not determined for poor solubility.

3. Results and discussion

3.1. Polymer synthesis and characterization

Table 1 summarizes the conditions and results of the polymerization of L-phenylalanine- and L-serine-derived monomers LP and LS catalyzed with (nbd)Rh$^+$[η^6-$C_6H_5B^-(C_6H_5)_3$] in THF (Scheme 1). In the polymerization, (nbd)Rh$^+$[η^6-$C_6H_5B^-(C_6H_5)_3$] successfully afforded the polymers with moderate molecular weights (M_n = 4400–14,800) in good yields. The copolymers and poly(LS) were soluble in common organic solvents including MeOH, $CHCl_3$, AcOEt, DMF, DMSO and THF, while poly(LP) was partly soluble in these solvents. LP did not polymerize to achieve a homopolymer with high M_n and high solubility under this condition, which should be due to strong steric hindrance and repulsion caused by the excess bulky phenyl rings in the neighboring pedants. The specific rotations of the PAs measured at room temperature ranged from −120° to −386° in $CHCl_3$, which depended on the composition of the PAs. The absolute values of $[a]_D$ of polymers was about 40–96 times as large as that of monomers at the maximum, indicating that chiral amplification occurred. The large specific rotations of the copolymers demonstrated that the PAs might take preferred single-handed helical conformations. Furthermore, as far as the yields and M_n of the polymers concern, it could be inferred that hydroxyl group in LS did not hamper the polymerization which was consistent with previous reports [34–36], but promoted some of the PAs to form more stable and orderly helical structures.

The structures of the PAs were examined by ^{1}H NMR spectroscopy. The disappearance of the chemical shift assigned to the acetylene proton at about 2.2 ppm of all the PAs indicated that the monomers had been consumed by the polymerization reaction. However, the peaks corresponding to the resonances of the protons of the polyene backbone were hardly recognized for the broad proton signals around 4–6 ppm. Since Rh zwitterion complex commonly afford monosubstituted PAs with *cis*–transoidal structure [38], we assume that the steric structures of the present polymers are also this case.

The thermal stability of the PAs was investigated by TGA techniques under a nitrogen atmosphere from 50 to 600 °C. As shown in Fig. 1, the TGA curves for dry PAs exhibit a smooth, stepwise manner, suggesting a two-step thermal degradation. The onset temperatures (T_0) of weight loss of the polymers were all above 200 °C, indicating considerably high thermal stability of the monosubstituted PAs. The temperatures of the onset and 5% weight loss (T_0, T_5) of the PAs have also been calculated by means of thermograms and used as criterion for evaluation of thermal stability of these PAs (Table 2). The decomposition temperatures for the polymers containing more phenylalanine moieties are higher than those containing more serine moieties, revealing that the incorporation of phenyl groups in the PAs can improve their thermal stability.

3.2. Hydrogen bonding of the PAs

Hydrogen bonds are an essential and fundamental interaction to form and maintain the helical structure of the amino acid-based PAs. Participation in hydrogen bonding decreases the frequency of free N—H and C=O vibrations but increases the intensities, making the absorption features useful in investigating hydrogen bonds [12,15]. The solution state FT-IR spectra of the monomer and polymer samples are examined to determine the existence of hydrogen bonding in the PAs. Fig. 2A shows the FT-IR spectra of LP, LS, and poly(LP_{50}-*co*-LS_{50}) (other copolymers see in Fig. S3). In $CHCl_3$, LP and LS showed the amide and carbamate absorption at 1705 and

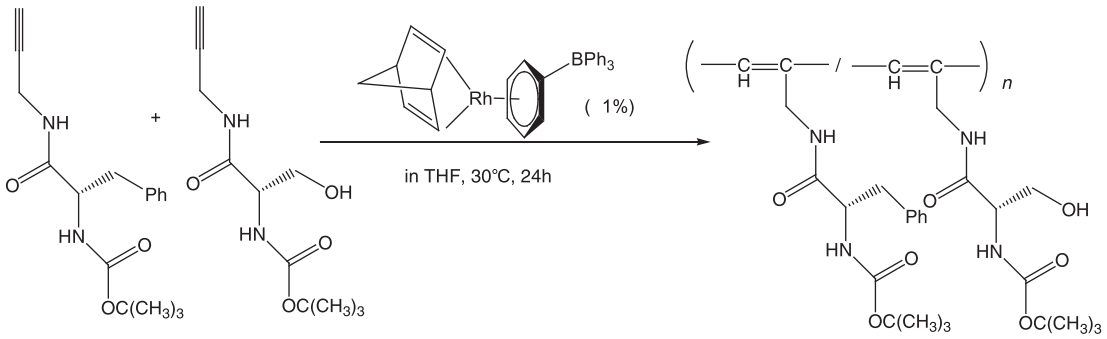

Scheme 1. Synthesis of the PAs.

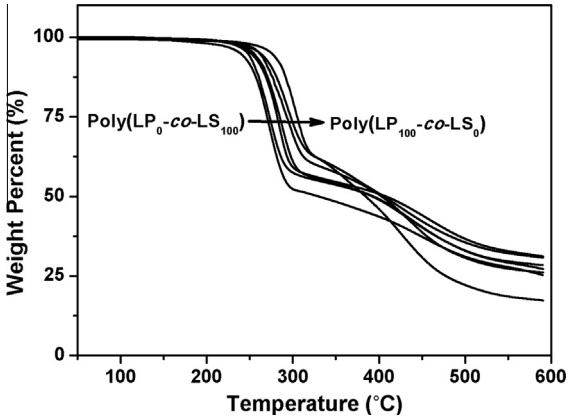

Fig. 1. TGA curves of the PAs.

Table 2
Thermal properties of the PAs.

Monomer feed ratio (LP:LS)	Onset decomposition temperature (°C) T_0	Decomposition temperature (°C) T_5
100:0	255	275
75:25	236	264
62.5:37.5	235	261
50:50	220	253
37.5:62.5	219	250
25:75	215	248
0:100	201	238

1678 (1675) cm^{-1}, while poly(LP_{50}-*co*-LS_{50}) exhibited two corresponding absorption peaks at 1698 and 1658 cm^{-1}. From the frequency decease of both the carbonyl groups, it can be concluded the PA partly forms inter- and/or intramolecular hydrogen bonds at amide and carbamate groups. As previously described, the intramolecular hydrogen bonding in the acid amino-based PAs dominantly stabilize the helical structure, while intermolecular hydrogen bonding may have the opposite effect. To further validate the kinds of the formed hydrogen bonds, the solution FT-IR spectra of poly(LP_{50}-*co*-LS_{50}) at different concentrations is also conducted in $CHCl_3$ as an example. As can be seen in Fig. 2B, with the decrease of the concentrations from 5 to 0.5 mM, the absorptions of hydrogen bonded N—H groups decreased together with the increasing amount of free N—H groups, indicating the disappearance of formed intermolecular hydrogen bonding. Besides, the absorption bands of carbonyl groups also became narrower. Interestingly, an obvious red-shift from 1698 to 1705 cm^{-1} of the band corresponding to carbamate groups was observed upon the decreasing concentration, while no frequency shift occurred at the band of amide. When the concentration was below 0.5 mM, there was no significant difference at the absorption bands of carbonyl groups. However, but even at such low concentrations, still high degree of hydrogen bonding derived from the N—H and C=O in amide groups existed, indicating the existence of intramolecular hydrogen bonding. Summarizing the observations in the FT-IR spectra (Table S1), it can be inferred that most of carbamate groups are probably participated in the formation of intermolecular hydrogen bonds, while the inner amide groups prefer to form intramolecular hydrogen bonds in the PAs.

3.3. Helical conformation of the PAs

Fig. 3 shows the CD and UV–vis spectra of the PAs measured at room temperature in $CHCl_3$. All the PAs obviously exhibited Cotton effect in the corresponding UV–vis absorption wavelength except poly(LP), which was hard to measure for its poor solubility. Poly(LP_{75}-*co*-LS_{25}) exhibited a CD signal at ~295 nm with negative sign which confirmed the existence of single-handed helical conformation. Poly($LP_{62.5}$-*co*-$LS_{37.5}$) and poly(LP_{50}-*co*-LS_{50}) also showed Cotton effects around 300 nm with negative signs similarly to poly(LP_{75}-*co*-LS_{25}), but intensified gradually, manifesting the formation of more stable but slightly looser helical structures. In the case of poly($LP_{37.5}$-*co*-$LS_{62.5}$) to poly(LS), positive signals appeared and shifted to lower wavelength, while the negative signals shifted to higher wavelength and the intensities gradually decreased. The positive and negative CD signals of poly(LS) centered at ~280 nm and ~345 nm, respectively. The change of the CD signs with the content of LS from 50% to 100% represented unstable and much looser helices in the PAs and we could further infer that the helical structure of these PAs might be formed in different ways. From the fact of CD spectra, poly(LP_{50}-*co*-LS_{50}) was examined to have the most stable and compact helical secondary structure among all the polymers. Additionally, during the course of CD variation phenomenon, the PAs all exhibited an absorption peak around 320 nm which was assigned to the main chain conjunction. Compared with reported amino acid-based PAs [27,28], it is further confirmed that hydroxyl group containing PAs have relatively more compact helical structures. No obvious difference in the absorption spectra was observed in the absorption spectra of PAs with different composition. Consequently, it can be concluded that the main chain conjunction in the PA backbone changes slightly with changing composition, but its two-dimensional spatial structure, especially the torsional angle of the alternating double bonds dramatically changes.

Since the helical PAs belong to dynamic helical polymers, it is likely that external stimuli such as heat and solvents can influence the formation and stabilization of their helical structure. The helix sense can be manipulated continuously by different solvents and this can help to understand the effect of phenyl and hydroxyl groups in controlling the helix of the PAs. As shown in Fig. 4, the

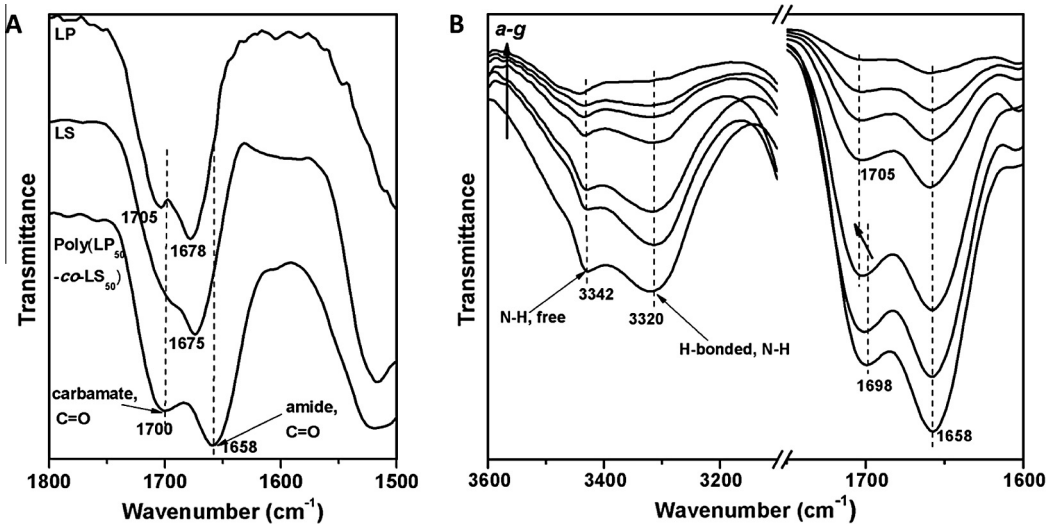

Fig. 2. (A) Solution FT-IR spectra of LP, LS, and poly(LP_{50}-*co*-LS_{50}) in $CHCl_3$ (c = 1 mM). (B) Solution FT-IR spectra of poly(LP_{50}-*co*-LS_{50}) in $CHCl_3$ at the concentrations of (a) 5 mM, (b) 2.5 mM, (c) 1 mM, (d) 0.5 mM, (e) 0.25 mM, (f) 0.1 mM, and (g) 0.05 mM.

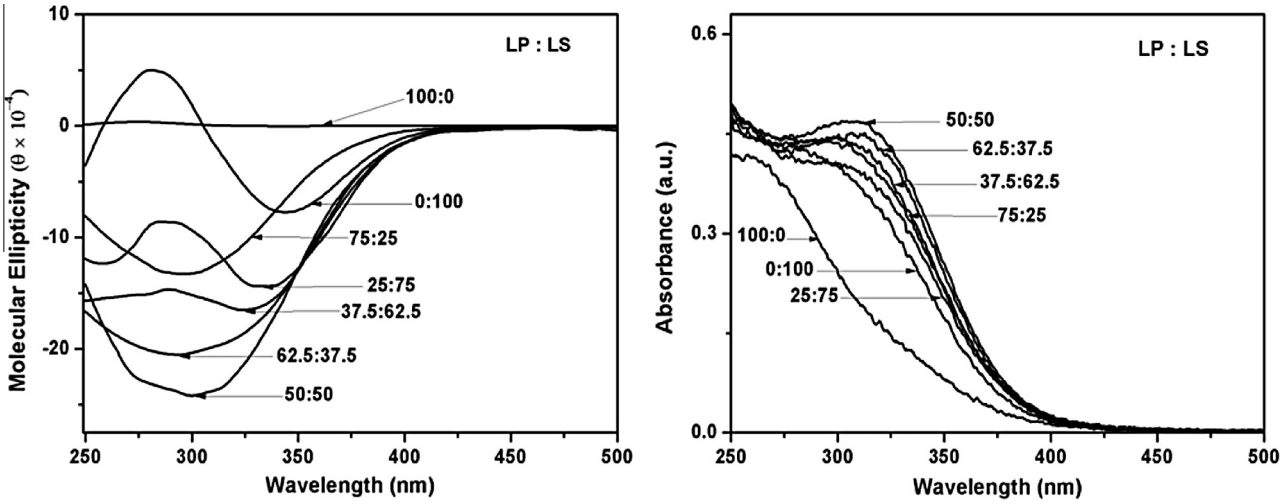

Fig. 3. CD and UV–vis spectra of the PAs measured in $CHCl_3$ at room temperature (c = (0.73–1.01) mM).

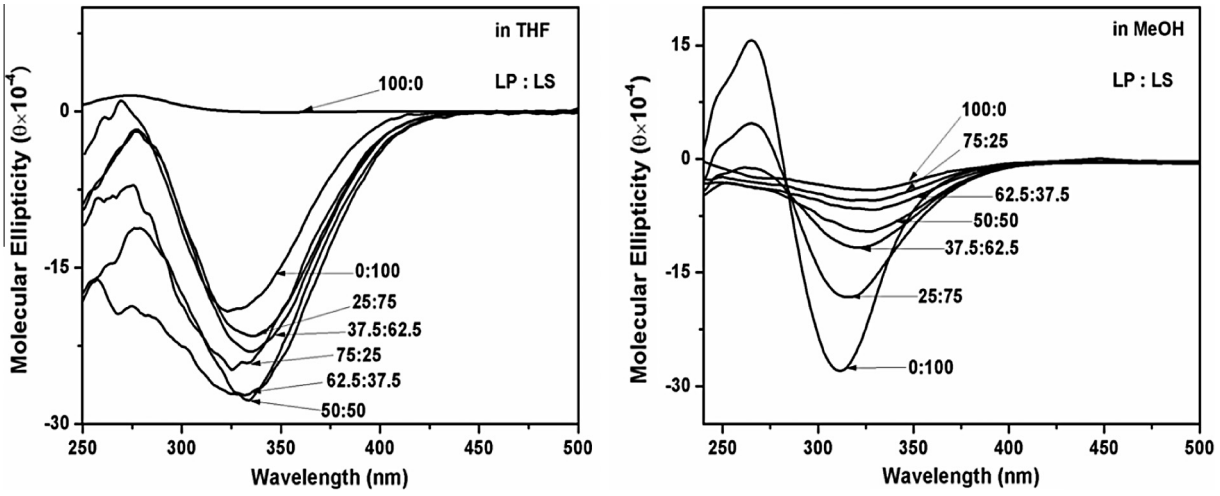

Fig. 4. Solvent effect on the CD spectra of the PAs measured in THF and MeOH (c = (0.73–1.01) mM).

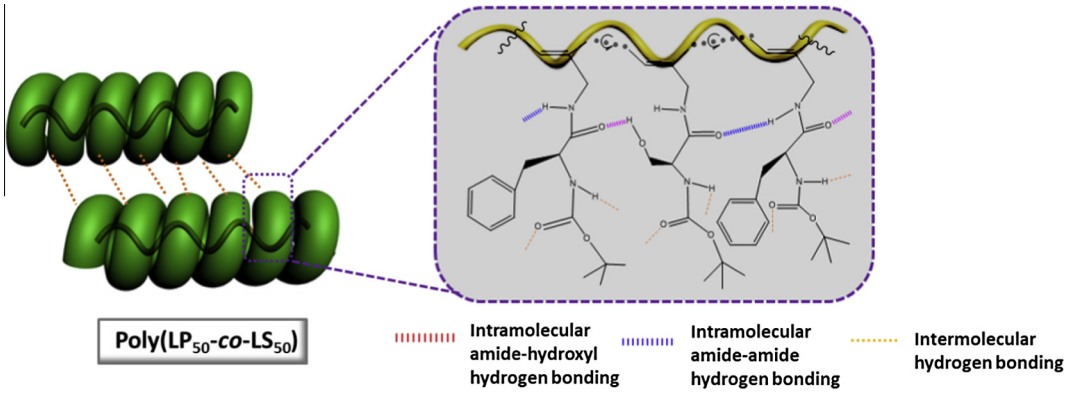

Fig. 5. Helical conformation and hydrogen bonding of typical pitches in poly(LP_{50}-*co*-LS_{50}) chains.

Table 3
Infrared emissivity values of the PAs at room temperature.

Monomer feed ratio (LP:LS)	Infrared emissivity ε_{25} (8–14 μm)
100:0	0.964
75:25	0.751
62.5:37.5	0.697
50:50	0.632
37.5:62.5	0.705
25:75	0.793
0:100	0.825

solvent effect on the helical secondary structure of the PAs was estimated by CD spectra in THF and MeOH. In THF, the CD signals of the all PAs appeared at ~325 nm and similar tendency of the stability was observed as in $CHCl_3$, indicating that the helical structure formed in a similar way. On the other hand, the PAs in MeOH shows quite different Cotton effect. In MeOH, the positive and negative CD signals around 270 and 310 nm suggest that the PAs also take helical structure. However, with the increasing proportion of LS, the intensities of both the negative and positive signals underwent a corresponding increase, which confirmed that the hydroxyl group played an important role in the forming the secondary structure of the macromolecules. Since the helical conformation is likely to be stabilized by intramolecular hydrogen bonding along with steric repulsion, strong polar or protic solvents may change its helicity and stability by influencing the formation of hydrogen bonds to change asymmetric forces between substitutes. For THF, the strong polarity can affect the hydrophobic interaction of the bulky phenyl groups in the side chains to decrease the asymmetric forces of the main chain to loose the helix and provide more possibility to form hydrogen bonds [27,28,39]. In addition, MeOH can shield the inner amide groups by preventing them to form intramolecular hydrogen bonds with hydroxyl groups [34–36]. Thence, it is not hard to assume that hydroxyl groups participate in forming intramolecular hydrogen bonds with inner amide groups and the ratio of LP and LS is important in controlling the helix. Furthermore, the CD intensities of PAs in different solvents varied greatly, although the concentration of each PA was approximately equivalent. The $[\alpha]_D$ values measured in MeOH were also different from those in $CHCl_3$ which were consistent with the CD spectra. For instance, the $[\alpha]_D$ of poly(LP_{50}-*co*-LS_{50}) in MeOH is −93°, which was much smaller than the value in $CHCl_3$ (−386°, in Table 1). These observations also agree with the fact that the hydroxyl group has significant effect in controlling and stabilizing the helix of the amino acid-based PAs.

By combining previous reports [31,35,36,40], information about the formation and stabilization of the helix in the PA can be interpreted as follows: Since the extremely compact helix in poly(LP) is generated by amide-amide intramolecular hydrogen bonds and strong hydrophobic interactions between the neighboring phenyl groups in side chains [40], the incorporation of LS can increase the spacer length of the neighboring phenyl groups to relieve the hydrophobic interactions and provide PAs with moderate molecular weights. Besides, the hydroxyl group in the side chain is prefer to form inner amide–hydroxyl intramolecular hydrogen bonds to release the helix and increase its stability [35,36]. As LS increases from 0% to 50% in poly(LP-*co*-LS)s, hydrophobic interactions between the neighboring phenyl groups gradually weaken which in turn result in less compact helical structure. Meanwhile, part of the amide–amide intramolecular hydrogen bonds firmly converts to amide–hydroxyl hydrogen bonds which also have some effect in the decrease of helicity. Nevertheless, we find that the stability of helix increases largely which may be due to the weakened stereo-hindrance effect of bulky substituents and more convenient formation of hydrogen bonds. When the content of LS is raised further from 50% to 100%, steric effects between the substituents weaken rapidly because of the decreasing amount of phenyl groups and more easy formation of intramolecular amide–hydroxyl hydrogen bonds. This eventually makes the helix much looser. Owing to more short side chains, intermolecular hydrogen bonds constructed between hydroxyl, carbamate, and other groups are widely formed which results in unpromising decrease in the helical stability [41]. In general, poly(LP_{50}-*co*-LS_{50}) has taken the most stable helical conformation with a relatively high helicity and it can be assumed that the competition effect on conformation between the steric factors and hydrogen bonding is controlled by the ratio of the two monomers and it will reach an optimal balance state of stability when the ratio comes to 1:1. Additionally, the structure information and hydrogen bonding formation of poly(LP_{50}-*co*-LS_{50}) is also in good agreement with the MMFF94 simulation (Fig. S5). The typical pitches in poly(LP_{50}-*co*-LS_{50}) chains is also schematically illustrated in Fig. 5, although exact structure information still remains not so clear.

3.4. Infrared emissivity analysis of the PAs

The infrared emissivity values of the as-prepared PAs at wavelength of 8–14 μm measured at room temperature are shown in Table 3. The infrared emissivity values of the PAs vary from 0.632 to 0.964. As mentioned in the Introduction, the vibration of unsaturated groups in PAs in the polymer chain brings about high infrared emissivity values. Closely packed pitches in the polymers are favored over the decrease the index of hydrogen deficiency and the unsaturated degree, thus reducing the infrared emissivity. As stable and compact helical structure improves the orderliness of molecules, the effective optimization of orderliness of the helix

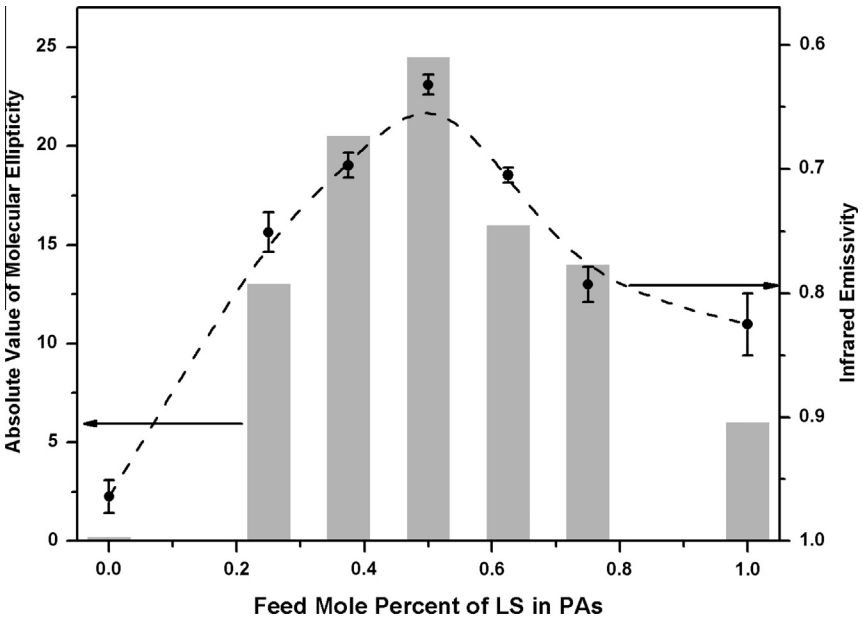

Fig. 6. Dependence of the infrared emissivity and Cotton effect intensity on the feed ratio of monomers.

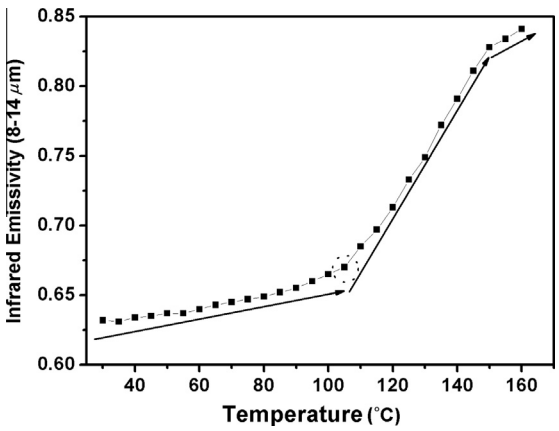

Fig. 7. Infrared emissivity values of poly(LP_{50}-*co*-LS_{50}) at 30–160 °C.

in PAs significantly contributes to the decrease in infrared emissivity. By combining data of the infrared emissivity values and their optical activities of the PAs in Fig. 6, empirical evidence has shown positive correlation between well-ordered and compact helical secondary structures and lower infrared emissivity values. Poly(LP_{50}-*co*-LS_{50}) which possesses the most orderly and compact helix has the lowest infrared emissivity. This has confirmed our assumption on the correlation between the secondary structure of helical polymer and their infrared emissivity in previous reports.

Furthermore, to further validate the effect of temperature on infrared emission, the infrared emissivity values of poly(LP_{50}-*co*-LS_{50}) measured from 30 to 160 °C were investigated and presented in Fig. 7. From 30 to 105 °C, the infrared emissivity value of poly(LP_{50}-*co*-LS_{50}) has increased slowly to 0.670; however, above 105 °C, the value is increased much more rapidly. There is an obvious inflectional point at about 105 °C and the infrared emissivity value is as high as 0.828 at 150 °C. These observations indicate that a large number of intramolecular hydrogen bonds have gradually disappeared above 105 °C and this may force the PA chain to adopt a randomly coiled conformation. As the orderliness and helicity of poly(LP_{50}-*co*-LS_{50}) decrease rapidly, the infrared emissivity dramatically increases at a high speed. Moreover, this result also proves that the importance of the participation of intramolecular hydrogen bonds in maintaining the helix of the PAs.

4. Conclusion

In summary, we have designed and synthesized a series novel optically active PAs derived from chiral phenylalanine and serine. The (co)polymers carrying proportional phenyl and hydroxyl groups in the side chains have shown unique features in their optical and thermal properties. Systematic experimental investigations have been carried out to determine the roles of hydrogen bonding and steric factors in stabilizing the helical structure of the PAs. The infrared emissivity values of the PAs have been measured and the correlation between the infrared emissivity and secondary structure has been captured. The results show that the improvement of the stability and helicity of the helical structure in organic polymers significantly contributes to the decrease in infrared emissivity. Among these polymers, poly(LP_{50}-*co*-LS_{50}) shows the lowest infrared emissivity ($\varepsilon_{25} = 0.632$) value and excellent resistance against heat ($\varepsilon_{105} = 0.670$), which have met the requirements of common use. Therefore, the incorporation of the chiral amino acid in the resulting PAs provides a great promise in the development of polymers with tunable infrared emissivity. Overall, the application of PAs in reducing infrared emission in this paper is important not only because they exemplify extend application of helical polymers, but also because they provide a novel method to develop materials with low-emissivity.

Acknowledgements

The authors are supported by National Nature Science Foundation of China (51077013), Key Program for the Scientific Research Guiding Found of Basic Scientific Research Operation Expenditure of Southeast University (Grant No. 3207043101) and Instrumental Analysis Fund of Southeast University, Fund Project for Transformation of Scientific and Technological Achievements of Jiangsu Province of China (No. BA2011086), the Innovation Research Foundation of College Graduate in Jiangsu Province (CXLX12-0107), and

the Scientific Research Foundation of Graduate School of Southeast University (YBJJ1417).

Appendix A. Supplementary material

Supplementary data associated with this article can be found, in the online version, at http://dx.doi.org/10.1016/j.reactfunctpolym.2014.05.006.

References

[1] C.X. Pan, J.Z. Zhang, Y. Shan, Appl. Therm. Eng. 51 (2013) 529–538.
[2] S.P. Mahulikar, H.R. Sonawane, G.A. Rao, Prog. Aerosp. Sci. 43 (2007) 218–245.
[3] B.V. Bergeron, K.C. White, J.L. Boehme, A.H. Gelb, P.B. Joshi, J. Phys. Chem. C 112 (2008) 832–838.
[4] L. Chen, C. Lu, Z. Fang, Y. Lu, Y. Ni, Z. Xu, Mater. Lett. 93 (2013) 308–311.
[5] K.S. Chou, Y.C. Lu, Thin Solid Films 515 (2007) 7217–7221.
[6] B. Lin, H. Liu, S. Zhang, C. Yuan, J. Solid State Chem. 177 (2004) 3849–3852.
[7] B. Lin, J. Tang, H. Liu, Y. Sun, C. Yuan, J. Solid State Chem. 178 (2005) 650–654.
[8] H. Yu, G. Xu, X. Shen, X. Yan, C. Cheng, Appl. Surf. Sci. 255 (2009) 6077–6081.
[9] J. Chen, Y.M. Zhou, Q.L. Nan, Y.Q. Sun, X.Y. Ye, Z.Q. Wang, Appl. Surf. Sci. 253 (2007) 9154–9158.
[10] T. Nakano, Y. Okamoto, Chem. Rev. 101 (2001) 4013–4038.
[11] E. Yashima, K. Maeda, H. Iida, Y. Furusho, K. Nagai, Chem. Rev. 109 (2009) 6102–6211.
[12] H. Zhao, F. Sanda, T. Masuda, J. Polym. Sci. Part A: Polym. Chem. 45 (2007) 1691–1698.
[13] M. Banno, T. Yamaguchi, K. Nagai, C. Kaiser, S. Hecht, E. Yashima, J. Am. Chem. Soc. 134 (2012) 8718–8728.
[14] Y. Furusho, E. Yashima, Macromol. Rapid Commun. 32 (2011) 136–146.
[15] Z.Q. Wang, Y.M. Zhou, Y.Q. Sun, Q.Z. Yao, Macromolecules 42 (2009) 4972–4976.
[16] Y. Yang, Y.M. Zhou, J.H. Ge, Y.J. Wang, X.L. Chen, Polymer 52 (2011) 3745–3751.
[17] Y. Yang, Y.M. Zhou, J.H. Ge, X.M. Yang, React. Funct. Polym. 72 (2012) 574–579.
[18] Y. Yang, Y.M. Zhou, J.H. Ge, Y.J. Wang, Y.X. Zhu, J. Solid State Chem. 184 (2011) 2617–2622.
[19] J. Qu, Y. Suzuki, M. Shiotsuki, F. Sanda, T. Masuda, Macromol. Chem. Phys. 208 (2007) 1992–1999.
[20] S. Etemad, T. Mitani, M. Ozaki, T.C. Chung, A.J. Heeger, A.G. MacDiarmid, Solid State Commun. 40 (1981) 75–79.
[21] Y.M. Huang, J.W.Y. Lam, K.K.L. Cheuk, W. Ge, B.Z. Tang, Macromolecules 32 (1999) 5976–5978.
[22] R. Inoue, T. Kanaya, T. Masuda, K. Nishida, O. Yamamuro, Macromolecules 45 (2012) 6008–6014.
[23] R.P. Megens, G. Roelfes, Chem. Eur. J. 17 (2011) 8514–8523.
[24] J.W.Y. Lam, B.Z. Tang, Acc. Chem. Res. 38 (2005) 745–754.
[25] J. Liu, J.W.Y. Lam, Chem. Rev. 109 (2009) 5799–5867.
[26] T. Masuda, J. Polym. Sci. Part A: Polym. Chem. 45 (2007) 165–180.
[27] H. Zhao, F. Sanda, T. Masuda, Macromolecules 37 (2004) 8888–8892.
[28] H. Zhao, F. Sanda, T. Masuda, Macromolecules 37 (2004) 8893–8896.
[29] J. Qu, F. Sanda, T. Masuda, Eur. Polym. J. 45 (2009) 448–454.
[30] B.S. Li, K.K.L. Cheuk, D. Yang, J.W.Y. Lam, L.J. Wan, C. Bai, B.Z. Tang, Macromolecules 36 (2003) 5447–5450.
[31] B.S. Li, K.K.L. Cheuk, L. Ling, J. Chen, X. Xiao, C. Bai, B.Z. Tang, Macromolecules 36 (2002) 77–85.
[32] B.S. Li, J.W.Y. Lam, Z.Q. Yu, B.Z. Tang, Langmuir 28 (2012) 5770–5774.
[33] B.S. Li, K.K.L. Cheuk, F. Salhi, J.W.Y. Lam, J.A.K. Cha, X. Xiao, C. Bai, B.Z. Tang, Nano Lett. 1 (2001) 323–328.
[34] H. Zhao, F. Sanda, T. Masuda, J. Macromol. Sci. Pure Appl. Chem. 44 (2007) 389–394.
[35] F. Sanda, H. Araki, T. Masuda, Macromolecules 38 (2005) 10605–10608.
[36] F. Sanda, H. Araki, T. Masuda, Macromolecules 37 (2004) 8510–8516.
[37] R.R. Schrock, J.A. Osborn, Inorg. Chem. 9 (1970) 2339–2343.
[38] M. Shiotsuki, F. Sanda, T. Masuda, Polym. Chem. 2 (2011) 1044–1058.
[39] H. Zhao, F. Sanda, T. Masuda, Macromol. Chem. Phys. 207 (2006) 1921–1926.
[40] J. Deng, J. Tabei, M. Shiotsuki, F. Sanda, T. Masuda, Macromolecules 37 (2004) 9715–9721.
[41] J. Deng, J. Tabei, M. Shiotsuki, F. Sanda, T. Masuda, Macromolecules 37 (2004) 1891–1896.